LYMPHOID NEOPLASIA

Exosomes released by chronic lymphocytic leukemia cells induce the transition of stromal cells into cancer-associated fibroblasts

Jerome Paggetti,[1] Franziska Haderk,[2] Martina Seiffert,[2] Bassam Janji,[1] Ute Distler,[3] Wim Ammerlaan,[4] Yeoun Jin Kim,[3] Julien Adam,[5,6] Peter Lichter,[2] Eric Solary,[6,7] Guy Berchem,[1,8] and Etienne Moussay[1]

[1]Laboratory of Experimental Hemato-Oncology, Luxembourg Institute of Health, Luxembourg, Luxembourg; [2]Department for Molecular Genetics, German Cancer Research Center, Heidelberg, Germany; [3]Luxembourg Clinical Proteomics Center, Luxembourg Institute of Health, Luxembourg, Luxembourg; [4]Integrated BioBank of Luxembourg, Luxembourg, Luxembourg; [5]INSERM U981, Gustave Roussy, Villejuif, France; [6]Faculty of Medicine, University Paris-Sud, Le Kremlin-Bicêtre, France; [7]INSERM UMR1009, Gustave Roussy Villejuif, France; and [8]Centre Hospitalier de Luxembourg, Luxembourg, Luxembourg

Key Points

- CLL-derived exosomes are internalized by stromal cells, deliver functional microRNA and proteins, and activate key signaling pathways.
- Stromal cells exposed to CLL-derived exosomes demonstrate a CAF-like phenotype and secrete factors promoting CLL cell survival.

Exosomes derived from solid tumor cells are involved in immune suppression, angiogenesis, and metastasis, but the role of leukemia-derived exosomes has been less investigated. The pathogenesis of chronic lymphocytic leukemia (CLL) is stringently associated with a tumor-supportive microenvironment and a dysfunctional immune system. Here, we explore the role of CLL-derived exosomes in the cellular and molecular mechanisms by which malignant cells create this favorable surrounding. We show that CLL-derived exosomes are actively incorporated by endothelial and mesenchymal stem cells ex vivo and in vivo and that the transfer of exosomal protein and microRNA induces an inflammatory phenotype in the target cells, which resembles the phenotype of cancer-associated fibroblasts (CAFs). As a result, stromal cells show enhanced proliferation, migration, and secretion of inflammatory cytokines, contributing to a tumor-supportive microenvironment. Exosome uptake by endothelial cells increased angiogenesis ex vivo and in vivo, and coinjection of CLL-derived exosomes and CLL cells promoted tumor growth in immunodeficient mice. Finally, we detected α-smooth actin–positive stromal cells in lymph nodes of CLL patients. These findings demonstrate that CLL-derived exosomes actively promote disease progression by modulating several functions of surrounding stromal cells that acquire features of cancer-associated fibroblasts. (*Blood*. 2015;126(9):1106-1117)

Introduction

Chronic lymphocytic leukemia (CLL) is the most prevalent leukemia affecting adults and remains an incurable disease with current therapies. Mature CD5-positive B cells gradually accumulate in the blood and lymphoid organs. Although CLL has long been considered a relatively static disease, recent studies demonstrated that, through a constant recirculation of leukemic cells to bone marrow and lymph nodes, CLL is a more dynamic disease than previously thought.[1] CLL lymphocytes are clonal, based on immunoglobulin heavy chain gene rearrangement, but acquired somatic mutations were recently detected, demonstrating molecular heterogeneity[2] and an oligoclonal disease.[3,4] Circulating monoclonal CLL cells infiltrate the lymph nodes and bone marrow where they establish physical contacts with stromal cells[5,6] necessary to support their localization, proliferation, and survival.[7]

Extracellular vesicles represent a new component of this supportive microenvironment, are released by malignant cells and play an important role in cancer cell communication with their environment.[8-11] Exosomes are small vesicles (50-150 nm) generated via an endocytic pathway and are expressing chaperones (HSP70, HSP90) and tetraspanins (CD9, CD63, CD81). Exosomes contain proteins, DNA, noncoding RNAs, and mRNAs, and specific sorting mechanisms were proposed for loading selected molecules into exosomes.[12-14] Exosome uptake induces phenotypic changes in target cells as exosome miRNAs can silence mRNA targets and influence cellular functions.[15] Exosomes released by acute myeloid leukemia cells affect the proliferation and migration of bone marrow (BM) stromal cells,[16,17] multiple myeloma exosomes enhance angiogenesis,[18] melanoma-derived exosomes reprogram the BM niche to support metastasis,[19] and miR-105 conveyed by breast cancer-derived exosomes destroys the endothelial barrier to promote metastasis.[20] In CLL, circulating exosomes may affect mesenchymal stem cells (MSCs) and endothelial cells (ECs), which are both present in the BM and lymphatic tissues, where they support leukemic cell survival[21,22] and are possible sources of cancer-associated fibroblast (CAF).[23,24] Here, we report a comprehensive analysis of exosomes derived from CLL cells and their role in the dialogue between leukemic cells and their microenvironment. More specifically, we show that CLL cells induce stromal cells to adopt a CAF phenotype, thereby creating a niche promoting CLL cell adhesion, survival, and growth.

Submitted December 17, 2014; accepted June 16, 2015. Prepublished online as *Blood* First Edition paper, June 22, 2015; DOI 10.1182/blood-2014-12-618025.

The online version of this article contains a data supplement.

There is an Inside *Blood* Commentary on this article in this issue.

The publication costs of this article were defrayed in part by page charge payment. Therefore, and solely to indicate this fact, this article is hereby marked "advertisement" in accordance with 18 USC section 1734.

Materials and methods

Clinical samples

This research was approved by the Comité National d'Ethique de Recherche (Luxembourg, N°200903/02 and N°201211/11), and participants gave written informed consent in accordance with the Declaration of Helsinki.

Twenty-one CLL patients with a median age of 69.0 years (range, 52-88 years) were included in the study (supplemental Table 1 available on the *Blood* Web site). All patients had an absolute lymphocyte count >30 000/μL and were untreated for 3 months. Mononuclear cells and plasma were prepared as described before.[25,26] The proportion of CLL cells was always >95%. Human BM-MSCs were isolated as described before.[27]

Exosome isolation

Primary CLL cells and cell lines were used for exosome production. Typically, 300×10^6 primary CLL were cultured in 20 mL AIM-V medium (Invitrogen) and stimulated with 10 μg/mL anti-human immunoglobulin (Ig)M for 3 days. Cell lines were grown at similar density (20-40 $\times$ 10^6/mL) in CELLine flasks. Culture supernatants or plasma were harvested, sequentially centrifuged (supplemental Figure 1) to remove cells and debris (2×10 minutes at 400*g*, followed by 2×20 minutes at 2000*g*), and filtered (0.45 μm) to remove small debris and larger vesicles. Exosomes were isolated by ultracentrifugation (70 minutes at 110 000*g*, 4°C) followed by floatation on Optiprep cushion (Axis-Shield, 17%) for 75 minutes at 100 000*g* and 4°C to remove nonexosomal proteins complexes. After phosphate-buffered saline (PBS) wash, exosomes were suspended in PBS and filtered (0.45 μm).

Immunoblotting and antibody arrays

Immunoblotting was performed as previously described.[28] Phospho-kinases, cytokine, and angiogenesis arrays (R&D Systems) were used according to the manufacturer's instructions.

RNA analysis

Cellular and exosomal RNA were isolated using the miRCURY RNA Isolation Kit (Exiqon). MicroRNA quantitative reverse transcriptase-polymerase chain reaction (qRT-PCR) detection was performed using TaqMan assays (Life Technologies).[27] Small RNAs were analyzed by next-generation sequencing on Illumina Miseq Sequencer after library preparation using NEBNext Multiplex Small RNA Library Prep Set for Illumina Set 1 (New England Biolabs). Gene expression was determined using the GeneChip Human Gene 1.0 ST Array platform (Affymetrix).

Flow cytometry analysis

Exosome phenotyping was performed using a BD Influx following published recommendations.[29] Cell phenotyping and measure of Rituximab binding to CLL cells were performed using a BD FACSCanto.

Animal experiments

All experiments involving laboratory animals were conducted in a pathogen-free animal facility with the approval of the Luxembourg Ministry for Agriculture. Mice were treated in accordance with the European Union guidelines. For the mouse tumor model, subcutaneous xenograft transplantations were performed as previously reported.[30] Eight-week-old NSG mice were challenged subcutaneously in the flank with 5×10^6 MEC-1-eGFP cells supplemented with 200 μg CLL exosomes.

Statistics

Data are presented as mean ± standard deviation. Statistical significance was determined using *P* values based on Student *t* tests (2-tailed; $\alpha < 0.05$). Significance displayed in each figure is explained in figure legends.

Accession number

Microarray data are available at ArrayExpress (experiment: E-MTAB-2765). Small RNA next-generation sequencing data are available at http://www.ebi.ac.uk/ena/data/view/PRJEB6780.

Results

CLL exosomes are actively incorporated by MSCs, ECs, and myeloid cells in vitro and in vivo

On coculture of PKH67-labeled primary CLL cells with BM-MSCs in culture inserts for 24 hours, we observed a transfer of membrane vesicles from CLL cells to BM-MSCs (Figure 1A; supplemental Figure 1A). To determine whether exosomes are released from CLL cells and may play a role in their communication with BM-MSCs or other cells within CLL microenvironment, we established an isolation protocol based on serial centrifugation, density-based separation, and filtration to purify exosomes from supernatant of CLL cells and exclude contamination by other vesicle types and protein aggregates (supplemental Figure 1B). Exosomes derived from the MEC-1 CLL cell line (referred as CLL exosomes) were used throughout this study, with key observations validated using exosomes derived from stimulated primary CLL cells (referred as primary CLL exosomes). Isolated particles presented bona fide characteristics of exosomes, ie, cup-shaped appearance in electron microscopy (Figure 1B), enrichment for exosome marker proteins ALIX/PDCD6IP, TSG101, HLA-DR, RAB5A, CD63, and CD81 but absence of calnexin in the respective density fraction of 1.15 to 1.17 g/mL (Figure 1C; supplemental Figure 1C-D), a size distribution of 70 to 200 nm (Figure 1D), and acetylcholine esterase activity (supplemental Figure 1E). Importantly, plasma of CLL patients exhibited an increased level of the exosome marker CD63 compared with healthy donor plasma (supplemental Figure 1F). Plasma exosomes showed similar size and protein markers (supplemental Figure 1G-H).

Purified CLL exosomes were labeled with PKH67 and added to HS-5 stromal or HMEC-1 endothelial cell lines at concentrations resembling those found in plasma of cancer patients.[31,32] Exosomes uptake was observed 1 hour after application, and exosomes accumulated in recipient cells over time, whereas no transfer was observed on incubation at 4°C (Figure 1E). Further, preincubation of exosomes with proteinase K or trypsin abrogated exosome transfer to stromal cells (supplemental Figure 1I). Both temperature dependence and involvement of specific proteins point toward an active exosome uptake mechanism. Interestingly, treatment of exosomes with heparin, a heparan sulfate analog, prior to their application to recipient cells also inhibited uptake by target cells, indicating an involvement of heparan sulfate proteoglycans (HSPGs) in this process (Figure 1F). Furthermore, we observed that CLL exosomes enter all the tested cell types except CLL B cells. When PKH67-labeled MEC-1 exosomes were added to culture, endothelial, stromal, and multiple myeloma cells, but not CLL cells (green line), acquired PKH67 fluorescence, indicating exosome uptake (supplemental Figure 1J). Consistent with this, we detected 4 common HSPGs (syndecan-1 and -2 and glypican-1 and -3) on the surface of MSCs and ECs but not CLL cells, potentially explaining why CLL exosomes do not enter CLL cells (supplemental Figure 1J).

We then identified exosome target cells in vivo by intravenously injecting PKH26-labeled exosomes in mice. Within 18 hours after injection, exosome accumulate in $CD31^+$ cells in bone marrow, peripheral blood leukocytes, spleen, and liver (supplemental Figure 2A). Application of exosomes to murine BM cells revealed that endothelial progenitors, myeloid cells, and BM-MSCs are the major populations

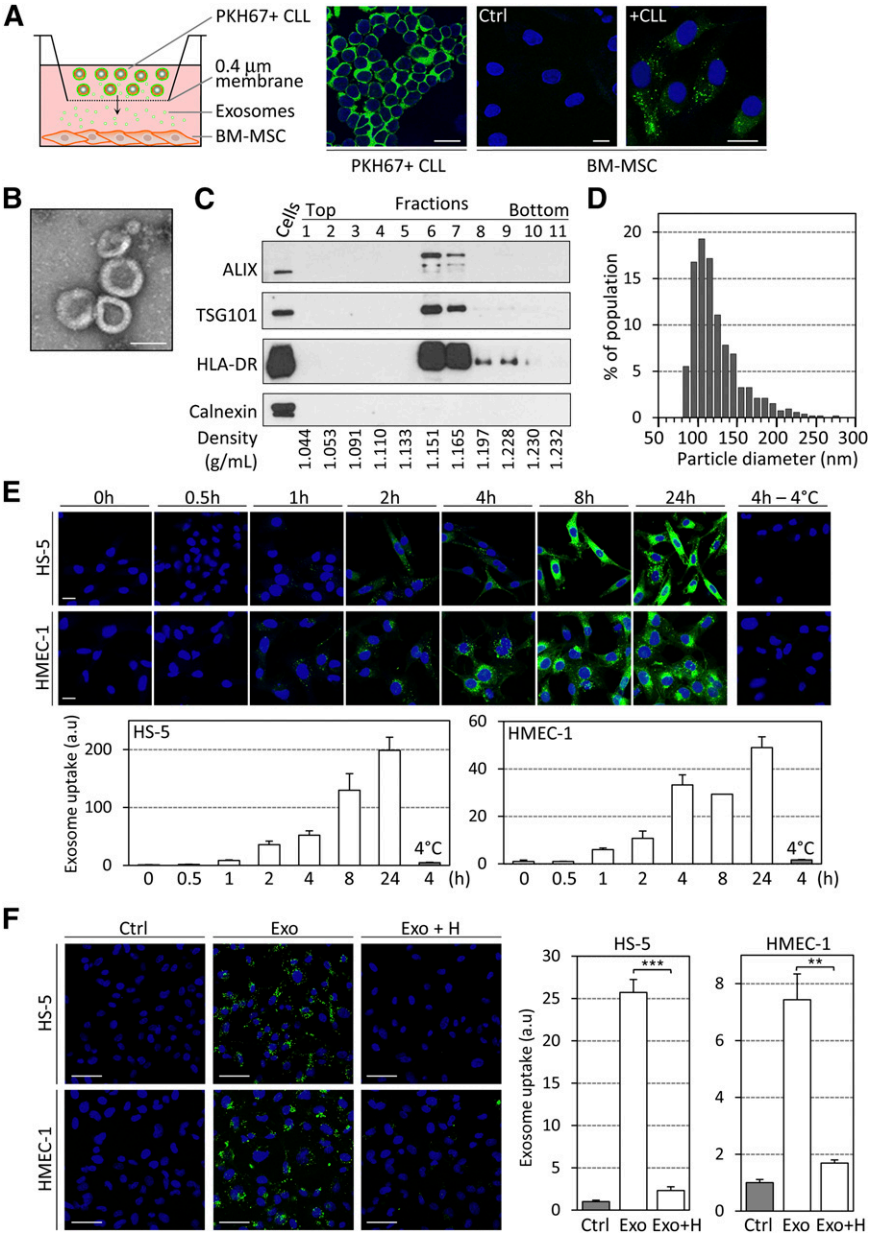

Figure 1. CLL cells secrete exosomes that rapidly enter stromal cells in culture. (A) A 24-hour coculture assay of primary CLL cells (1×10^6 in upper compartment) and BM-MSCs (2×10^4) was established in 6-well plates containing 0.4-μm pore inserts. BM-MSCs were cultured in the absence (Ctrl) or presence (+CLL) of primary PKH67-labeled CLL cells (green). Images were captured by fluorescence confocal microscopy. Nuclei were stained with 4,6 diamidino-2-phenylindole (DAPI) (blue). Representative image of n = 6 experiments. Scale bar, 20 μm. (B) Electron microscopy image of purified CLL exosomes. Scale bar, 100 nm. (C) Western blot analysis of the fractions collected after sucrose density gradient of the 110 000*g* pellets obtained using ultracentrifugation of CLL cell supernatants. Positive control was CLL cell lysate. (D) Size analysis of CLL exosomes using tunable resistive pulse sensing (TRPS)-based analysis (qNano). (E) The BM-derived stromal cell line HS-5 and the endothelial cell line HMEC-1 were incubated with 50 μg/mL PKH67-labeled CLL exosomes (MEC-1) for the indicated times before 4 washes and fixation. (Upper) Exosome uptake was followed by fluorescence confocal microscopy. Scale bar, 20 μm. (Lower) Quantification of exosome uptake by ImageJ software. Data are presented as fold change relative to 0 hours (n = 3). (F) HS-5 and HMEC-1 cells were incubated for 4 hours in the absence (Ctrl) or presence of 20 μg/mL PKH67-labeled CLL exosomes (MEC-1) untreated (Exo) or pretreated for 30 minutes with 10 ng/mL heparin (Exo + H). (Left) Images were captured by fluorescence confocal microscopy. Scale bar, 50 μm. (Right) Quantification of exosome uptake by ImageJ software. Data are presented as fold change relative to Ctrl (n = 3). $^{**}P < .01$, $^{***}P < .001$.

targeted by exosomes in the microenvironment (supplemental Figure 2B-C).

In summary, we show that CLL cells secrete exosomes, which are actively taken up in vitro and in vivo primarily by various benign cells present in the tumor microenvironment, including ECs, myeloid cells, and BM-MSCs.

CLL exosomes transfer functional microRNA and proteins to target cells

Next, we characterized RNAs and proteins shuttled via exosomes to identify possible functions of exosomes in the remodeling of CLL microenvironment. Comparing whole RNA lysates of CLL exosomes and CLL cells, a striking predominance of small RNA species and a lack of ribosomal RNAs was observed in exosomes (Figure 2A). Therefore, we performed small RNA sequencing, again comparing CLL exosomes and respective CLL cells (supplemental Table 2). Small RNA profiles indicated that miscellaneous RNAs (miscRNAs), ie, RNA sequences mapping to the human genome but not assigned to any RNA category, were particularly enriched in CLL exosomes (Figure 2B). Regulatory Y RNAs, which belong to a specific class of short noncoding RNAs required for DNA replication,[33] resemble the predominant fraction and account for 55% of all small RNA reads in CLL exosomes. We also detected 838 mature miRNAs in CLL exosomes with 276 miRNAs present with ≥1 read per million mappable miRNA reads. Among the latter, the 5 most abundant miRNAs (miR-21, miR-155, miR-146a, miR-148a, and let-7g) represented 65% of all miRNA reads (Figure 2C). Some of these miRNAs (miR-21, miR-155, and miR146a) were previously identified in our study focusing on circulating miRNA in CLL patients.[26] Further, miR-146a was specifically enriched in CLL exosomes compared with cells (ratio 15:1). The less abundant miR-451 had the highest exosome-to-cell content ratio (440:1) and was previously reported to be elevated in CLL plasma.[26] In conclusion, miRNA complexity in CLL exosomes is less than in cells, but exosome miRNAs account for a proportion of circulating miRNAs and might be of functional relevance when taken up by target cells.

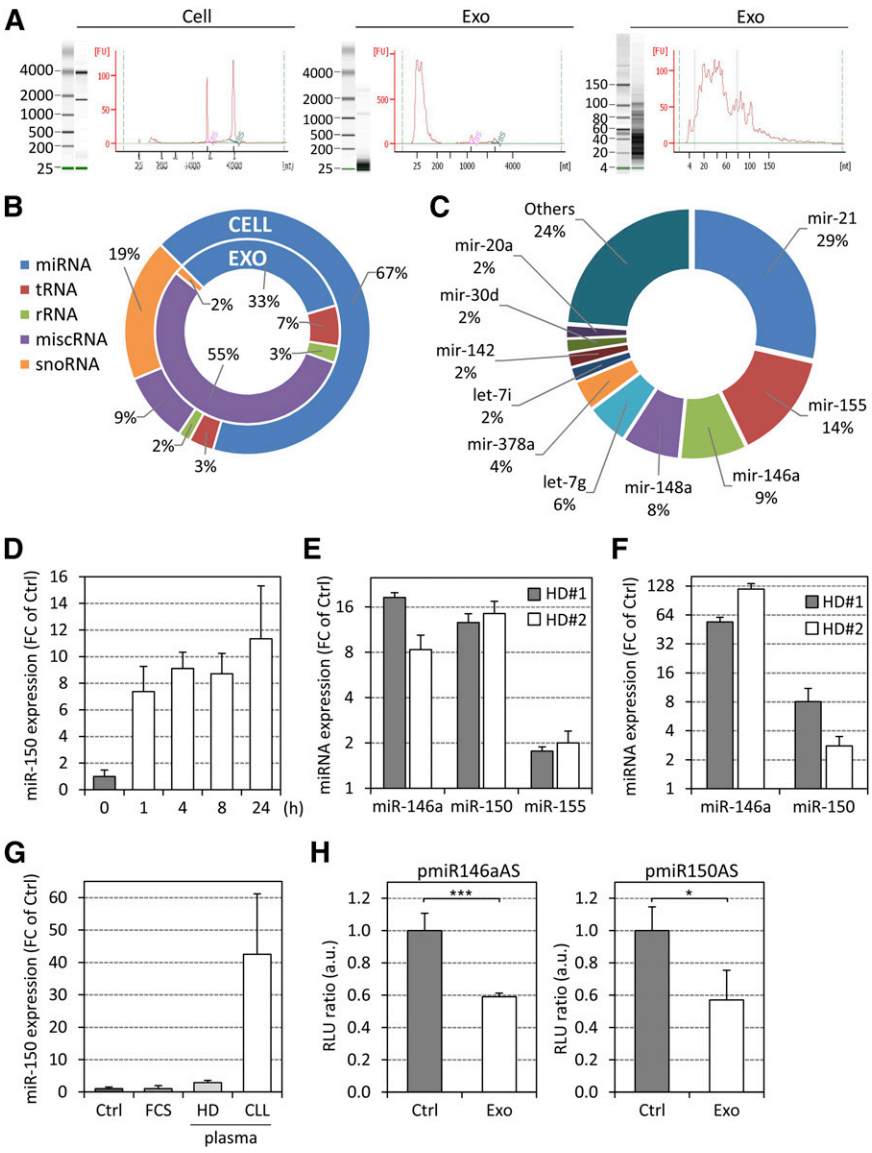

Figure 2. Characterization of CLL exosome RNA and transfer of functional miRNAs to target cells. (A) RNA was extracted from CLL cells and exosomes and analyzed using the Agilent Bioanalyzer RNA (left and middle) and small RNA (right) chips. (B and C) Small RNA next-generation sequencing of RNA purified from CLL cells and exosomes (MEC-1). (B) Percentages of the various small RNA categories identified in CLL cells and exosomes. (C) Percentages of the 10 most abundant miRNAs in CLL-exosomes. (D and E) Primary BM-MSCs from healthy donors (HD) were treated with 50 μg/mL CLL exosomes (MEC-1) for the indicated times, and specific miRNAs were quantified by qRT-PCR. Data are presented as fold change (FC) relative to untreated cells (Ctrl). (D) Kinetic quantification of miR-150 (n = 3). (E) Quantification of miR-146a, miR-150, and miR-155 after 72 hours. (F) Quantification of miR-146a and miR-150 in BM-MSCs (2×10^4) cocultured with primary CLL cells (1×10^6 in upper compartment) in 0.4-μm pore inserts for 24 hours by qRT-PCR. Data are presented as FC relative to BM-MSCs alone (Ctrl). (G) qRT-PCR quantification of miR-150 in BM-MSCs incubated with DMEM (Ctrl), DMEM supplemented with 20% fetal calf serum, HD, or CLL plasma for 3 hours (n = 3). (H) HMEC-1 cells were transfected with luciferase reporter plasmids carrying miR-146a or miR-150 antisense sequences (pmiR146aAS or pmiR150AS) and then cultured in the absence (Ctrl) or presence of MEC-1 exosomes (Exo) for 24 hours. Luciferase activity of reporter plasmid was quantified by measuring the light emission (RLU) of both luciferases in 4 replicates per condition. Data are presented as RLU ratio relative to Ctrl (n = 3). $^*P < .05$, $^{***}P < .001$.

Treatment of primary BM-MSCs with CLL exosomes resulted in an increase in miR-150 level, a miRNA very abundant in CLL plasma,[26] in cells 1 hour after exosome application. miRNA levels increased further over time (Figure 2D) comparably to vesicle accumulation in target cells (Figure 1E). Moreover, similar results were obtained for miR-146a and miR-155 when CLL exosomes were applied to BM-MSCs for 72 hours (Figure 2E). Further, a considerable increase in miR-146a and miR-150 levels was detected in BM-MSCs when cocultured with primary CLL cells in culture inserts (Figure 2F) and for miR-150 when cultured in Dulbecco's modified Eagle medium (DMEM) supplemented with 20% CLL plasma (Figure 2G). We validated that the increase in miRNA levels was due to transfer via CLL exosomes rather than induction of miRNA synthesis. On actinomycin D treatment, transcription of U6 and MYC was inhibited in cells, whereas an increase in miR-150 level was still observed on exosome application (supplemental Figure 3A). To demonstrate that exosome-derived RNAs are functional in target cells, we showed that stably expressed green fluorescent protein (GFP) could be silenced in cells incubated with CLL exosomes transfected with anti-GFP small interfering RNA (supplemental Figure 3B). This is strengthened by our finding that miR-146a and -150 were functional in target cells as demonstrated by luciferase reporter assays (Figure 2H).

Altogether, this suggests that miRNA candidates present in CLL exosomes and detected in CLL plasma[26] are transferred to target cells and functionally active, as exemplified here for the shuttling of miR-150 and miR-146a to BM-MSCs.

Besides the transfer of RNAs, exosomes are able to shuttle proteins to recipient cells, highlighting their potency in cell-cell communication due to multiple molecules simultaneously transferred. We characterized by mass spectrometry the proteome of exosomes isolated from primary CLL cells, MEC-1 and JVM-3 culture supernatants (supplemental Table 3). Ontology analysis showed an enrichment of proteins originating from various cell compartments including cell membrane, cytoplasm, and cytoskeleton (Figure 3A). Pattern recognition analysis also showed the enrichment of CLL exosomes in proteins displaying a KFERQ (Lys-Phe-Glu-Arg-Gln)-like motif (67% in exosome proteome vs 37% in cell proteome), which is implicated in targeting proteins to multivesicular bodies and thus pointing to specific sorting mechanisms for some exosome proteins. Thinking of possible phenotypic changes induced on exosome-mediated protein transfer, Ingenuity pathway

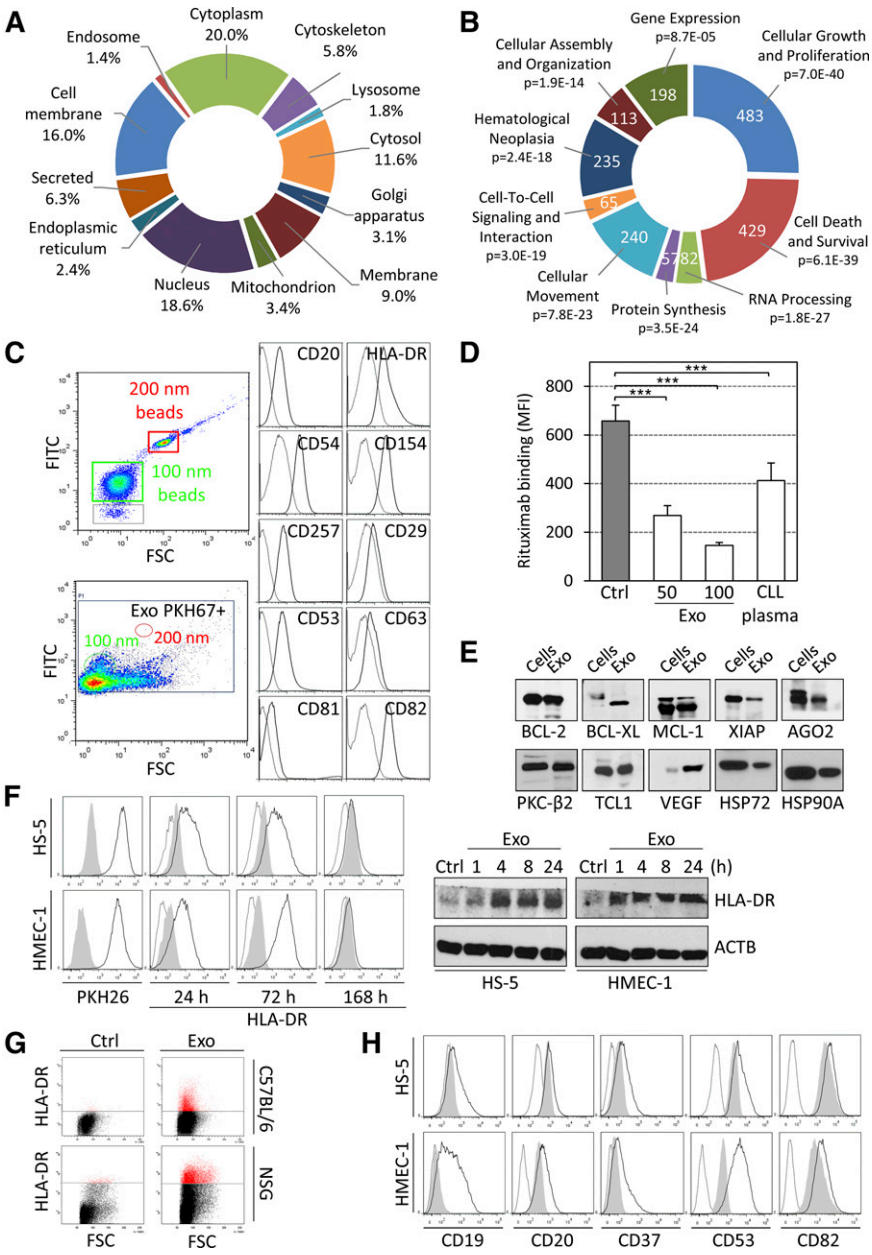

Figure 3. Proteomic characterization of CLL exosomes and transfer of proteins to target cells. (A and B) LC-MS/MS analysis of proteins extracts from CLL exosomes. (A) Subcellular localization of proteins identified in CLL exosomes (UniProt database). (B) Molecular functions associated with proteins identified in CLL exosomes (IPA). Portion radii were calculated according to the number of molecules associated with the functions. Cellular functions are indicated with their respective *P* values. (C) Phenotyping of individual CLL exosomes (MEC-1) was performed by flow cytometry. Exosomes were labeled with PKH67 and only green fluorescence-positive events were selected for analysis. The size of exosomes was confirmed using 100- and 200-nm beads. Exosomes were stained with indicated monoclonal antibodies (solid line) or with respective isotype controls (dotted line). (D) MEC-1 cells (10^5 in 100 μL) were treated with 2 μg/mL rituximab alone (Ctrl) or in combination with 50 or 100 μg/mL CLL exosomes (Exo) or with 30% (v/v) CLL plasma for 1 hour at 37°C. The binding of rituximab to CLL cells was followed by flow cytometry using an anti–rituximab-specific antibody. Data are presented as mean fluorescence intensities (MFIs; n = 3). ***$P < .001$. (E) Immunoblot analysis of proteins from CLL exosomes purified by Optiprep cushion. Lysate from CLL cells served as the control. (F) HMEC-1 and HS-5 cells were untreated (Ctrl, gray shade) or incubated with 50 μg/mL PKH26-labeled CLL exosomes (MEC-1; black line) for indicated periods of time, and the transfer of HLA-DR was followed by flow cytometry using specific antibody or isotype control (dotted line) (left). Results were confirmed using immunoblot (right). (G) C57BL/6 and NSG mouse BM cells were untreated (Ctrl) or incubated with CLL exosomes (MEC-1; 50 μg/mL) ex vivo for 24 hours. The transfer of human HLA-DR protein was followed using flow cytometry (representative of 3 animals). (H) HMEC-1 and HS-5 cells were untreated (gray shade) or incubated with 50 μg/mL CLL exosomes (MEC-1; black line) for 24 hours. Cells were analyzed by flow cytometry using specific antibodies or isotype controls (dotted line) to show the transfer of proteins from CLL exosomes to target cells (representative of n = 3).

analysis (IPA) showed the involvement of exosome proteins in cell proliferation, survival, migration, protein synthesis, and RNA processing (Figure 3B). Some of these pathways were studied in functional assays thereafter.

Analysis of CLL exosomes at the single-particle level[34] confirmed the presence of B cell-specific molecules, including CD20, and tetraspanins at the surface of individual exosomes (Figure 3C). We demonstrated a marked decrease in rituximab deposition on CLL cells in the presence of exosomes or plasma (Figure 3D), suggesting a role of CD20-bearing exosomes in the protection against rituximab. Finally, immunoblot analyses confirmed the presence of antiapoptotic proteins, angiogenic factors, RNA processing proteins, oncogenes, or heat shock proteins in CLL exosomes (Figure 3E).

Similar to RNA, exosome proteins were also transferred to recipient cells, as exemplified for human leukocyte antigen (HLA)-DR molecules shuttled via exosomes to stromal cells (Figure 3F-G). In addition, the transfer of B cell-specific markers (CD19 and CD20) and tetraspanins (CD37, CD53, and CD82) and their presentation at the surface of target cells were revealed by immunophenotyping (Figure 3H).

In conclusion, we provide compelling evidence that CLL exosomes transfer functional RNAs and proteins to recipient cells in amounts sufficient to alter intrinsic levels of respective molecules, thus possibly contributing to changes observed in nonmalignant cells of the CLL microenvironment.

CLL exosomes induce an inflammatory phenotype in stromal cells

We next evaluated the phenotypic changes induced by CLL exosomes and identified activated signaling pathways in BM-MSCs and ECs. An increased phosphorylation of several kinases was detected in target cells 1 hour after exosome treatment, among which RAC-alpha serine/threonine-protein kinase (AKT), extracellular signal-regulated kinase (ERK)1/2, C-AMP response element-binding protein (CREB), glycogen synthase kinase (GSK)3α/β, and others (Figure 4A). As

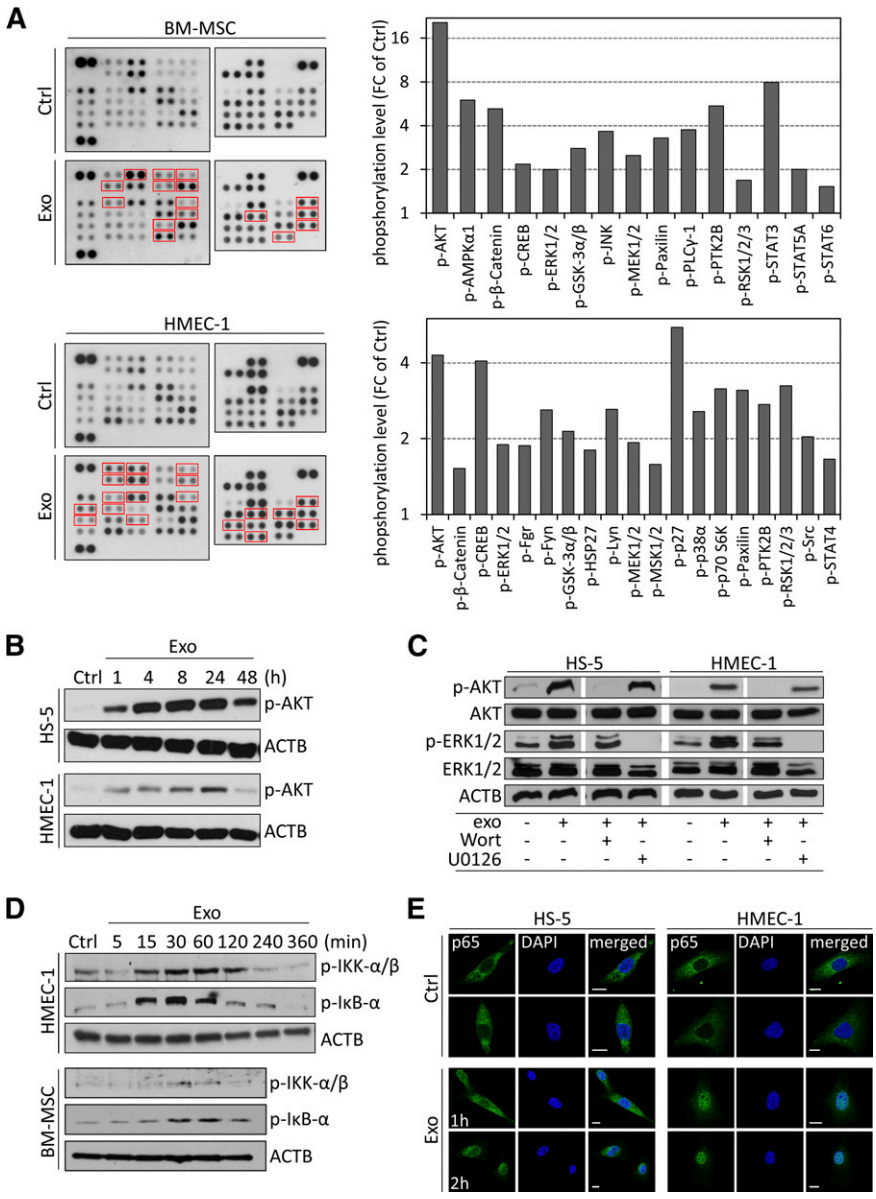

Figure 4. CLL exosomes rapidly activate kinases and NF-κB in stromal cells. (A) Phospho-kinase antibody array performed on protein lysates from BM-MSCs and HMEC-1 cells either untreated (Ctrl) or treated for 1 hour with 50 μg/mL CLL exosomes (MEC-1; Exo) (left). Cell lysates were hybridized to membranes containing capture antibodies specific for phosphorylated kinases. Quantification of CLL exosome-induced phosphorylated proteins highlighted by red boxes in left panel (right). Data are reported as fold change (FC) relative to Ctrl. (B) Kinetic of CLL exosome-induced AKT phosphorylation in HS-5 and HMEC-1 cells by immunoblot analysis. ACTB was used as loading control (representative of n = 3). (C) HS-5 and HMEC-1 were preincubated for 30 minutes in the absence (−) or presence (+) of PI3K inhibitor wortmannin (Wort, 100 nM) or MEK inhibitor U0126 (10 μM) before culturing for 5 minutes in the absence (−) or presence (+) of 50 μg/mL CLL exosomes (MEC-1). Expression of AKT and ERK1/2 and their phosphorylated forms (p-AKT and p-ERK1/2) was analyzed by immunoblot. ACTB was used as loading control (representative of n = 3). (D) Immunoblot analysis of IKK-α/β and inhibitory NF-κBα phosphorylation in cell lysates of BM-MSCs and HMEC-1 untreated (Ctrl) or incubated with 50 μg/mL CLL exosomes (MEC-1) for the indicated periods of time. ACTB was used as loading control (representative of n = 3). (E) Representative images of nuclear translocation of p65 in exosome-treated cells.HS-5 and HMEC-1 cells were untreated (Ctrl) or treated with CLL exosomes (Exo; 50 μg/mL) for 1 or 2 hours. After fixation and permeabilization, cells were labeled with anti-p65 antibody (green) and DAPI (blue) and analyzed by confocal microscopy (n = 3). Scale bar, 10 μm.

validated for AKT, phosphorylation was maintained for ≥24 hours (Figure 4B), indicating a strong and persistent activation of signaling cascades in target cells. Short-term treatment (5 minutes) with exosomes in the presence of AKT/ERK pathway inhibitors indicated that phosphorylation of kinases is caused by induction of protein phosphorylation rather than transfer of phosphorylated proteins (Figure 4C).

Because several kinases activated in target cells are closely associated with nuclear factor (NF)-κB signaling (eg, AKT and GSK3β), we evaluated a possible induction of NF-κB and found that inhibitor of kappa B kinase (IKK)α/β and inhibitory NF-κBα are phosphorylated 15 to 30 minutes after exosome application (Figure 4D), indicating the release of NF-κB from inhibitory IκBα. An immunofluorescent staining confirmed the rapid translocation of active p65/NF-κB into the nucleus (Figure 4E). In conclusion, CLL exosomes are able to activate different signaling cascades in target cells due to presentation and/or transfer of a multiplicity of RNAs and proteins, which finally results in subsequent changes in transcription factor activity.

Pointing to alterations in transcription factor activity mediated by CLL exosomes, gene expression may be affected in target cells. Gene expression profiling in primary BM-MSCs indicated the significant alteration at transcript level of 778 genes on exosome treatment (supplemental Table 4). Performing gene ontology analysis (IPA), we identified major changes in functions such as cell survival, migration and adhesion, proliferation, RNA expression, and inflammation (Figure 5A). CAFs are principal components of the tumor-supportive microenvironment in various cancers, and CLL is associated with an inflammatory milieu, leading to microenvironment-dependent regulation of cell proliferation. Therefore, an alteration of stromal cells toward a CAF phenotype is likely in CLL. Because CAF-mediated functions are strictly dependent on NF-κB signaling, we evaluated our transcriptome data set for changes in genes associated with CAF phenotype and performed unsupervised hierarchical clustering. A previously described, CAF gene expression signature[22,35] was observed in BM-MSCs treated with CLL exosomes (Figure 5B). Unsupervised clustering also identified expression changes in gene signatures related to cell growth, survival, movement, and inflammation in BM-MSCs (supplemental Figure 4A). qRT-PCR analysis followed by unsupervised hierarchical clustering confirmed the difference in expression of genes encoding

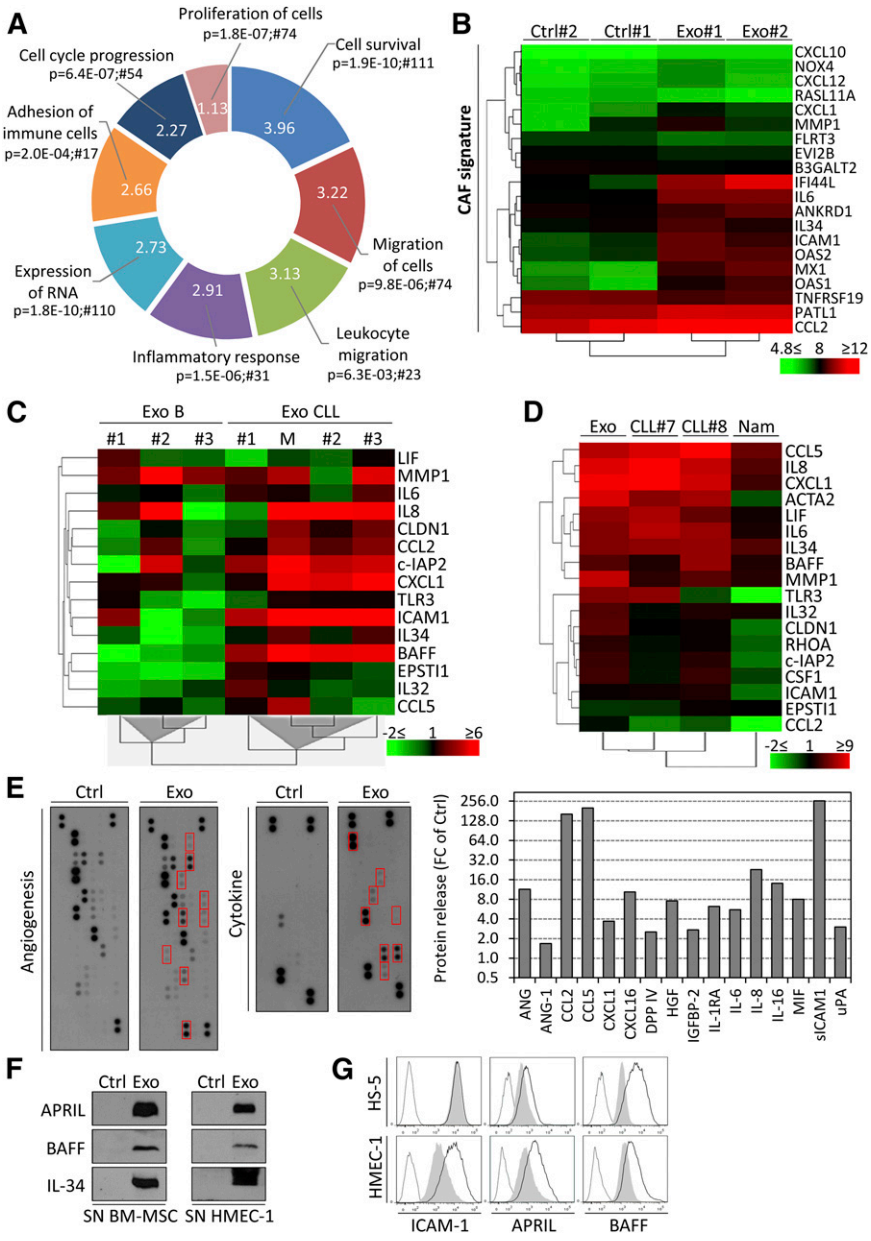

Figure 5. CLL exosomes alter the transcriptome of stromal cells and induce the release of cytokines and proangiogenic factors. (A) Primary BM-MSCs from 2 healthy donors were untreated (Ctrl) or treated with 50 μg/mL CLL exosomes (MEC-1; Exo) for 6 hours, and gene expression was analyzed by microarrays. Functions (IPA) associated with modulated genes are indicated with their respective *P* values and numbers of associated molecules. Portion radii were calculated according to *z* score, reflecting activation of the function. (B) CAF signature of BM-MSCs incubated with CLL exosomes. Normalized gene expression values (in log2) were used for unsupervised hierarchical clustering using the TM4MeV software. (C) Unsupervised hierarchical clustering based on gene expression of selected candidates from Figure 5B and supplemental Figure 4A. BM-MSCs were incubated for 72 hours with exosomes produced by healthy donor B cells (B, n = 3), primary CLL cells (CLL, n = 3), or MEC-1 cells (M). qPCR data are reported as fold change (log2 FC) relative to untreated cells. (D) Unsupervised hierarchical clustering based on gene expression of selected candidates from Figure 5B and supplemental Figure 4A. BM-MSCs were cultured for 30 days and stimulated weekly with 50 μg/mL CLL exosomes (MEC-1; Exo) or cocultured with 1×10^6 primary CLL cells (CLL#7 and CLL#8) or Burkitt's lymphoma Namalwa cell line (Nam) in culture inserts (0.4-μm pores). Medium and cells were changed twice weekly in the upper compartment. qPCR data are reported as fold change (log2 FC) relative to untreated cells. (E) Angiogenesis and cytokine antibody arrays used for the detection of soluble factors in the supernatants of untreated (Ctrl) or CLL exosome-treated (MEC-1; Exo; 50 μg/mL) BM-MSCs after 30 hours culture (left). Quantification of CLL exosome-modulated factors highlighted by red boxes in left panel (right). Data are reported as FC relative to Ctrl. (F) Immunoblot analysis of additional cytokines of interest not present in the arrays. Culture supernatants of BM-MSCs and HMEC-1 untreated (Ctrl) or treated with 50 μg/mL CLL exosomes (Exo) for 24 hours were concentrated and analyzed by immunoblot. (G) HMEC-1 and HS-5 cells incubated for 24 hours in absence (gray shade) or presence (black line) of 50 μg/mL CLL exosomes (MEC-1). Cells were then analyzed by flow cytometry with specific antibodies or isotype controls (dotted line) (representative of n = 3).

cytokines and chemokines (*IL8, BAFF, CXCL1, LIF*, *IL6*, *IL32*, *IL34*, *CCL2*, and *CCL5*), antiapoptotic factors (*c-IAP2*), and migration/invasion-related factors (*CLDN1*, *EPSTI1*, *ICAM1*, and *MMP1*) in BM-MSCs exposed to exosomes derived from primary CLL cells compared with healthy donor B cells (Figure 5C). Of note, several genes validated by qRT-PCR were already associated with the CAF gene signature (*CXCL1, IL6, IL34, CCL2, ICAM1,* and *MMP1*). A similar gene regulation was observed in BM-MSCs and endothelial cells treated with CLL exosomes (supplemental Figure 4B).

To recapitulate the secretion of CLL exosomes and their effects on BM-MSCs under more physiologic conditions, we established long-term cocultures (30 days) of BM-MSCs with primary CLL cells in culture inserts or treated BM-MSC weekly with exosomes. We performed similar experiments with the Burkitt lymphoma cell line Namalwa to investigate whether the impact on stromal cells is CLL specific. Gene expression analysis revealed that CLL exosomes and CLL cells cocultured in inserts induced similar gene expression changes in BM-MSCs, indicating that cell-cell contact was dispensable for the observed effects, highlighting the relevance of exosomes for microenvironment changes. Importantly, lymphoma cells induced a distinct gene expression pattern in BM-MSCs (Figure 5D), suggesting a specific response to CLL exosomes.

We next determined how changes in gene expression were translated into protein synthesis and secretion in the supernatant of BM-MSCs incubated with CLL exosomes. The increased levels in cytokines, chemokines, and proangiogenic factors (Figure 5E) confirmed a shift of BM-MSCs to a CAF phenotype on exosome treatment. A similar secretory profile was obtained for ECs treated with exosomes (supplemental Figure 5A), implying an overlap of targets in different recipient cell types. The presence of B-cell activating factor (BAFF) and interleukin-34 (upregulated in the gene expression profiling [GEP] data set), as well as A proliferation-inducing ligand (APRIL), was confirmed in supernatants of cells stimulated with primary CLL exosomes but not with exosomes

produced by healthy donor B cells (Figure 5F; supplemental Figure 5B). The level of BAFF, APRIL, and intercellular adhesion molecule-1 was also increased at cell surface (Figure 5G). We further observed an increased collagenase activity in stromal conditioned media (supplemental Figure 5C), confirming the induction of CAF phenotype by CLL exosomes.

In summary, stimulation by CLL exosomes results in a disease-specific response in target cells, thereby mimicking the multiplicity of effects induced by CLL cells themselves and having a strong impact on CLL microenvironment. As exemplified by major changes in the secretory profile of BM-MSCs and ECs in vitro, exosomes induce a shift toward a CAF phenotype, which might partly reflect the situation in CLL patients.

CLL exosomes induce proliferation and migration of stromal cells and angiogenesis ex vivo and in vivo

We next explored how changes in gene expression and protein synthesis induced by CLL exosomes affected stromal cells properties. On exosome treatment, we noticed a significant and dose-dependent increase in proliferation of stromal cells (Figure 6A), a significantly enhanced migration (Figure 6B), and a striking actin cytoskeleton remodeling in BM-MSCs. The latter was defined by the formation of stress fibers and α-smooth muscle actin (α-SMA) accumulation (Figure 6C), a characteristic of activated stroma and CAFs.[22,36] A similar formation of stress fibers was observed in stromal cells and fibroblasts, together with an increased expression of RhoA, a GTP-binding protein necessary for this actin skeleton remodeling (supplemental Figure 6A-C) when cells were incubated with exosomes. Exosomes produced by healthy donor B cells did not induce α-SMA expression (Figure 6C). Importantly, high levels of α-SMA–positive stromal cells were detected in infiltrated lymph nodes of CLL patients (Figure 6D), independently of the vasculature (supplemental Figure 7A), indicating the presence of CAFs in CLL. As angiogenesis is important in the pathology of CLL,[37] we also evaluated the impact of CLL exosomes on this process. CLL exosomes increased the formation of new aortic microvessels ex vivo (Figure 6E), favored the formation of endothelial tubes (Figure 6F; supplemental Figure 7B), and induced the formation of blood vessel in Matrigel plugs in vivo (Figure 6G).

Taken together, these results demonstrate that CLL exosomes exhibit a strong impact on stromal cell proliferation, actin cytoskeleton remodeling, migration, and angiogenesis: important characteristics of CAFs and means to remodel the microenvironment to promote tumor progression in malignancies,[38,39] as confirmed by the presence of CAFs in CLL lymph nodes.

CLL-derived exosomes enhance tumor growth in vivo

Finally, we investigated whether exosome-induced alterations in stromal cells impact on CLL cells and provide a benefit for disease development and progression. First, we evaluated in vitro whether exosomes influence adhesion of primary CLL cells to stromal cells and enhance CLL cell survival. Foremost, we observed increased CLL cell adhesion to exosome-treated stromal cells (Figure 7A), thereby implying a strengthened cell-cell interaction. Then we observed significantly increased survival rates of primary CLL cells cultured for 6 days in supernatants of exosome-stimulated BM-MSCs (Figure 7B), similarly to the effect of purified cytokines (Figure 7C), indicating that exosome-treated stromal cells have an enhanced capacity to support CLL cell survival. Therefore, the impact of CLL exosomes on tumor growth was studied in vivo by subcutaneously injecting MEC-1-eGFP cells[30] into immunocompromised NSG mice. Coinjection of cells with exosomes resulted in an increased tumor size compared with tumor cells injected without additional exosomes (Figure 7D). The accumulation of MEC-1-eGFP cells in mice kidneys (Figure 7E) also confirmed the renal involvement observed in CLL patients.[40,41] Our data demonstrate a protumorigenic effect of CLL-derived exosomes in vivo and their importance in the early onset of the disease when tumor cells impact the microenvironment to proliferate and promote angiogenesis, which is similar to previous studies.[19,20,42,43]

In summary, our in vitro and in vivo data show that CLL exosomes harbor an oncogenic potential by stimulating stromal cells to induce an inflammatory and protumorigenic milieu, including increased angiogenesis, thus supporting the survival and outgrowth of CLL cells.

Discussion

Increasing evidence indicates that the tumor microenvironment is not only a result of cancer development but rather contributes to it.[44] Novel drugs that target interactions of malignant cells with nonmalignant stromal cells, prevent adhesion or homing of tumor cells to specific niches, or block immune checkpoint regulatory proteins show encouraging results in clinical trials.[45,46] As exosomes are important mediators in the cross-talk of tumor cells with their microenvironment,[19] we need to understand their role and function in carcinogenesis to be able to interfere with their oncogenic properties. As their role in hematologic malignancies is largely unexplored, we aimed at characterizing, both molecularly and functionally, chronic lymphocytic leukemia-derived exosomes. A summary of our findings, suggesting a major contribution of exosomes to leukemogenesis by inducing the transition of stromal cells into CAFs, is depicted in supplemental Figure 8.

First, we show here that CLL-derived exosomes rapidly enter and deliver their content (specific miRNAs, Y RNAs, and proteins) to stromal cells (MSCs and ECs) through an active process requiring specific functional surface proteins (tetraspanins and integrins) and the presence of HSPGs on the surface of target cells. Indeed, exosome uptake is inhibited by low temperature, proteolytic cleavage of exosome surface proteins, and by coating of exosomes with the HSPG analog heparin. Our results confirm and extend previous findings in other models[47,48] and indicate that entry mechanisms used by CLL exosomes are likely common to cancer-derived exosomes. This might explain why CLL cells, which do not express the 4 common HSPGs, cannot incorporate CLL-derived exosomes, making them more prone to be internalized by and to deliver their content to cells in the surrounding microenvironment. In addition, our data show CD20 expression on CLL exosome surface. A portion of patients still fails to respond to anti-CD20 therapy.[49] Binding of the anti-CD20 antibody rituximab to exosomes might lower the quantity of rituximab available for binding to CLL cells. Thus, exosomes could exert a strong negative effect on anti-CD20 antibody-based immunotherapy. Whether CLL cells might be influenced by exosomes released by other cell types has not been investigated here and remains to be elucidated.

In response to their interaction with CLL exosomes, BM-MSCs and ECs acquire a CAF phenotype with enhanced proliferative and migratory properties in vitro. We also detected a high proportion of

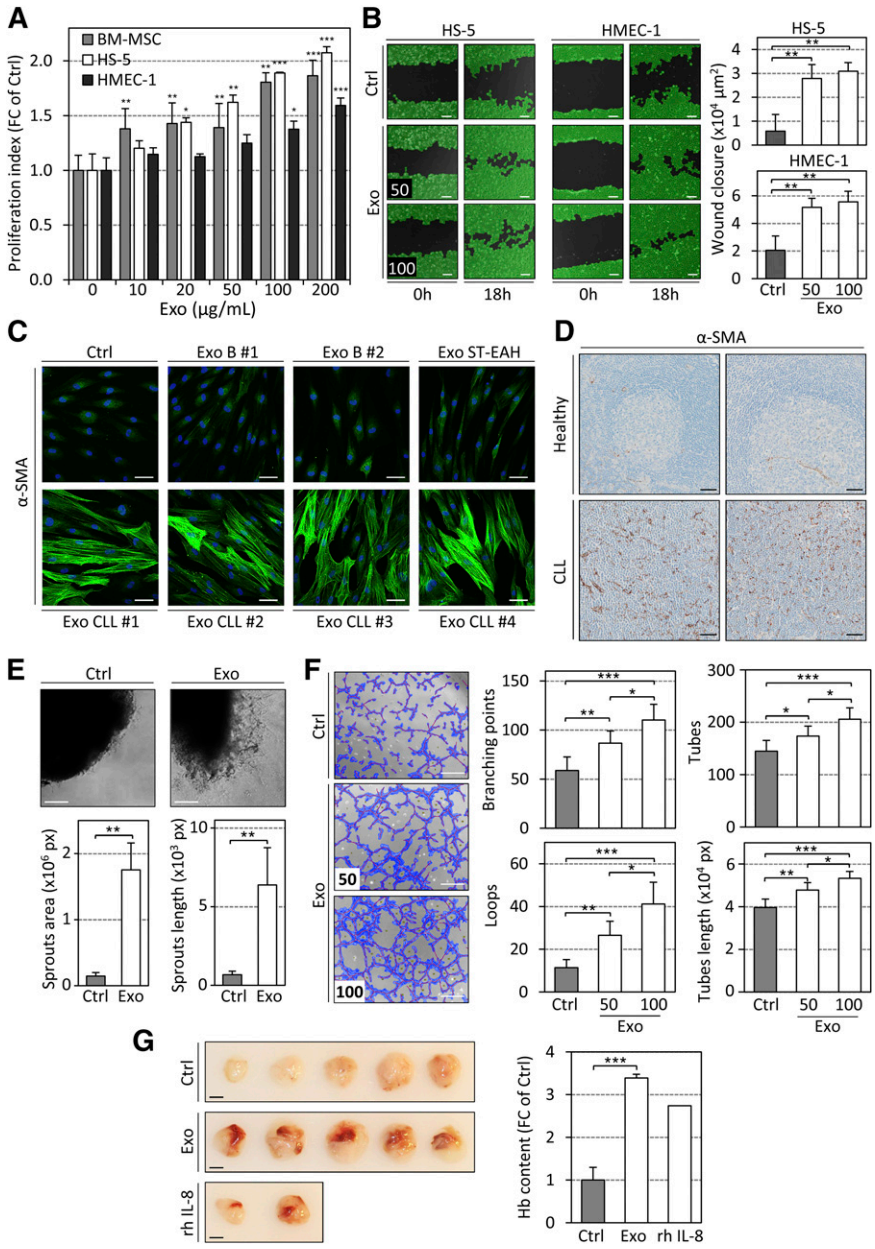

Figure 6. CLL exosomes promote cell proliferation, remodeling of the actin cytoskeleton, cell migration, and angiogenesis in vitro and in vivo. (A) Proliferation index of stromal cells after 96 hours of incubation with increasing concentrations of CLL exosomes (MEC-1) assessed using CCK8 assay. Data are reported as fold change (FC) of Ctrl (n = 4). $^{*}P < .05$, $^{**}P < .01$, $^{***}P < .001$. (B) Microscopy images of wound healing assay showing closure of the scratch when HS-5 or HMEC-1 cells were cultured in the absence (Ctrl) or presence (Exo) of 50 or 100 μg/mL CLL exosomes (MEC-1) in serum-free medium for 18 hours (left). Scale bar, 100 μm. Wound closure ($\times 10^4$ μm^2) was quantified from images using WimScratch (Wimasis; n = 4) (right). $^{**}P < .01$. (C) Representative images of immunofluorescence staining of α-SMA (green) in primary BM-MSCs untreated (Ctrl) or treated (Exo) for 15 days with exosomes produced by healthy donor B cells (B), lymphoblastoid cell line (ST-EAH), or primary CLL cells, captured by confocal microscopy (nucleus stained with DAPI, blue). Scale bar, 50 μm. (D) Representative images of immunohistochemistry staining of α-SMA in paraffin-embedded sections of human lymph nodes from 2 healthy individuals or 2 CLL patients (representative of n = 5). Scale bar, 50 μm. (E) (Upper) C57BL/6 mouse aorta pieces were incubated in vitro in the absence (Ctrl) or presence (Exo) of 100 μg/mL CLL exosomes (MEC-1) for 7 days. Representative microscopy images are shown. Scale bar, 100 μm. (Lower) Quantification of sprouts area and length using WimSprout (Wimasis; n = 4 replicates). $^{**}P < .01$. (F) (Left) HMEC-1 cells untreated (Ctrl) or treated for 30 minutes with 50 or 100 μg/mL CLL exosomes (MEC-1; Exo) and then seeded on Matrigel for 3 hours. Scale bar, 100 μm. (Right) Quantification of several parameters of the tube formation assay using WimTube (Wimasis; n = 4). $^{*}P < .05$, $^{**}P < .01$, $^{***}P < .001$. (G) Matrigel plug assay performed by subcutaneous injection of Matrigel mixed with PBS (Ctrl) or 100 μg of CLL exosomes (MEC-1; Exo) in 5 NSG mice. rhIL-8 was used as positive control. (Left) Images depict surgically removed Matrigel plugs after 14 days. Scale bar, 5 mm. (Right) Quantification of hemoglobin content in Matrigel plugs using Drabkin reagent. Data are reported as FC of Ctrl (n = 5). $^{***}P < .001$.

α-SMA–positive stromal cells in infiltrated lymph nodes of CLL patients, indicating the presence of CAFs in CLL in vivo. We propose that this phenotypic evolution to CAF, exemplified by the formation of actin stress fibers and a massive cytokine release, is, to a large extent, driven by a complex mixture of small RNAs and proteins contained by CLL exosomes. Among the cargoes identified in exosomes, tetraspanins can promote cell activation, growth, and motility,[50] and the most abundant miRNAs (miR-21 and -146a) are known critical regulators of CAF induction,[51,52] MSC proliferation,[53] and EC angiogenic activities.[54] On uptake of CLL exosomes, cell signaling pathways are activated, and gene expression is altered in target cells. Functionally, an increased expression of intercellular adhesion molecule-1 increases adhesion and incorporation of exosomes,[47] thereby leading to sustained activation and SRC kinase-dependent cytoskeletal remodeling.[55] Cellular activated pathways further induce specific protein phosphorylation in stromal cells (eg, p27 at residue T198), influencing protein localization and function and thus enhancing cell motility.[56]

Chronic inflammation is a hallmark of many cancers where cancer-associated fibroblasts together with tumor cells and immune cells contribute to trigger this inflammatory reaction.[38] Many proinflammatory cytokines identified in this study as secreted on exosome stimulation are also highly abundant in CLL patient serums, and their levels correlate with clinical stage and disease outcome. Indeed, some can directly enhance CLL cell survival,[57-59] promote CLL cell adhesion to stromal cells,[60] and regulate angiogenesis, thus potentially explaining the observed phenotypes of exosome-stimulated cells. Similarly, interleukin-34 released by stromal cells on exosome stimulation supports CLL cell survival and may contribute to the dialogue with surrounding myeloid cells.[61] Analysis of transgenic mouse models overexpressing APRIL or BAFF confirmed the importance of microenvironmental interactions in CLL development as these models developed aggressive forms of

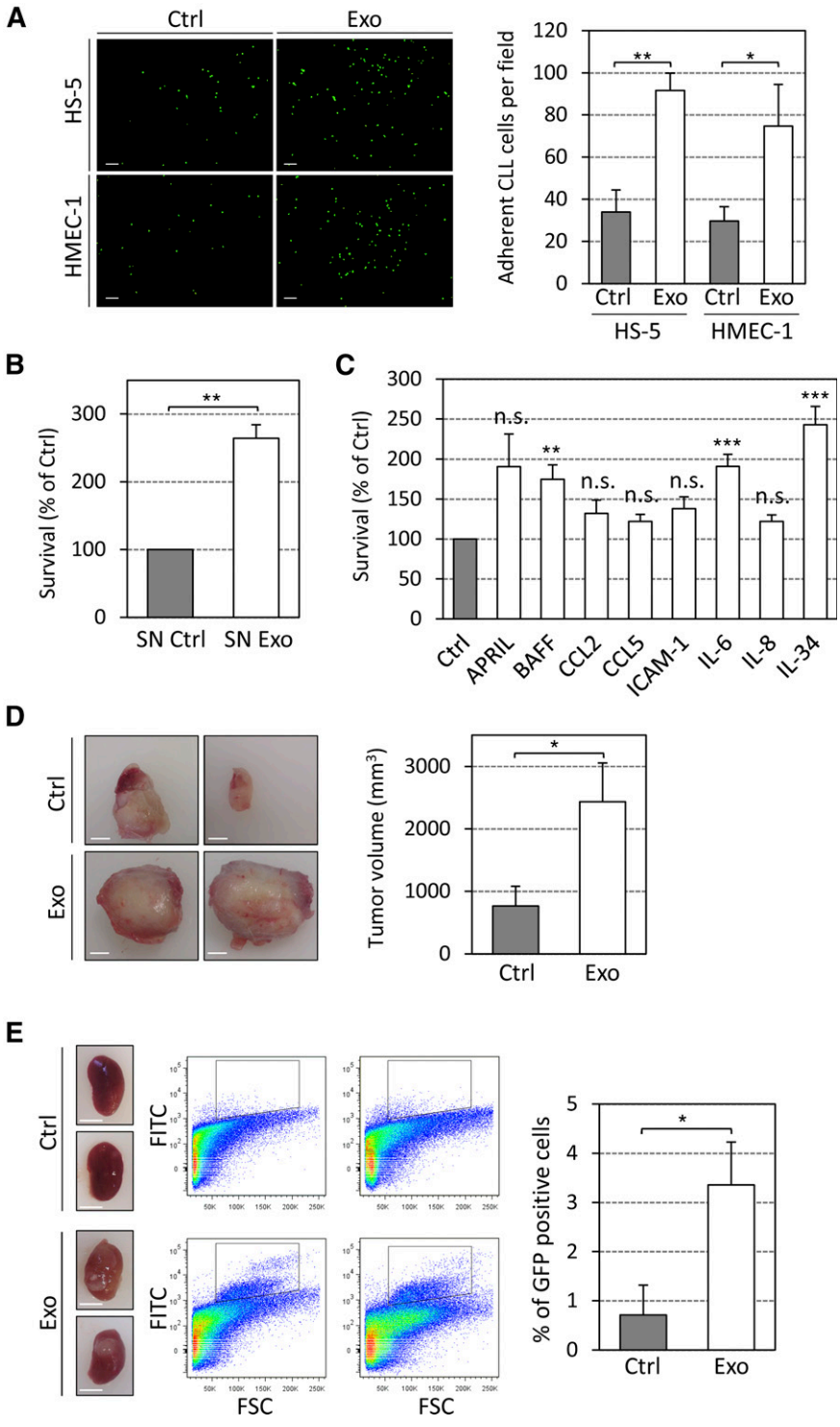

Figure 7. CLL exosomes increase CLL cell adhesion and survival in vitro and promote tumor growth in vivo. (A) Primary CLL cells labeled with PKH67 dye were added for 3 hours to cultures of HS-5 or HMEC-1 cells untreated (Ctrl) or pretreated 24 hours with 50 μg/mL of CLL exosomes (MEC-1; Exo). After 5 washes, images were taken via fluorescence microscopy. (Left) Representative images are shown. Scale bar, 100 μm. (Right) Quantification of CLL cell adhesion (n = 3). $^{*}P < .05$, $^{**}P < .01$. (B) CLL cells incubated with supernatants of BM-MSCs untreated (SN Ctrl) or treated for 24 hours with 50 μg/mL CLL exosomes (SN Exo). Cell viability was assessed after 6 days using CCK8 assay. Data are reported as the percentage relative to SN Ctrl (n = 3). $^{**}P < .01$. (C) Primary CLL cells were treated with indicated cytokines (10 ng/mL) and viability was assessed after 6 days using CCK8 assay. Data are reported as the percentage relative to Ctrl (n = 9). $^{*}P < .05$, $^{**}P < .01$, $^{***}P < .001$. (D and E) PBS (Ctrl) or 100 μg CLL exosomes (Exo) were mixed with 5×10^6 MEC-1-eGFP cells and subcutaneously injected into eight NSG mice. (D) (Left) Representative images of subcutaneous tumors removed from NSG mice. Scale bar, 5 mm. (Right) Quantification of tumor volume in mm^3. $^{*}P < .05$. (E) (Left) Representative images of kidneys (NSG mice). Scale bar, 5 mm. (Center) Representative flow cytometry plots showing MEC-1-eGFP cells (black gate) in kidneys. (Right) Quantification of GFP positive cells in kidneys.$^{*}P < .05$.

CLL with increased survival of CLL cells.[62] By secreting cytokines and chemokines, CAFs induce recruitment and retention of macrophages and other immune effector cells.[38] Of interest, CCL2 and CXCL16 induced by CLL exosomes are important chemoattractants for macrophages and T cells, respectively.[63,64] CAF-derived factors are known to modulate immune cell functions, skewing T cells and myeloid cells into immunosuppressive and tumor-promoting Th2/M2-like phenotypes. CCL2, CXCL1, and hepatocyte growth factor (HGF) were found to be elevated in serum of CLL patients vs healthy donors (M. Seiffert, unpublished data, 2014), indicating high clinical relevance. As CLL is a disease associated with defective T-cell and myeloid cell immune responses and an inflammatory milieu,[61,65] it is likely that CAFs residing within the BM and lymphoid organs contribute to these defects.

Even though the presence of CAFs was demonstrated in other malignancies,[38,39] how tumors induce these phenotypic changes in nonmalignant bystander cells remained unclear. Here we show that CAFs are also present in CLL lymph nodes and we and others show

that activation of AKT and NF-κB in stromal cells is essential to induce the inflammatory phenotype.[66] Our data suggest that exosomes are important mediators in this process and promote tumor growth in vivo. Ongoing studies will indicate whether targeting the interactions between exosomes and stromal cells could enforce the current therapeutic strategies.

Acknowledgments

The authors thank Dr L. Vallar, A. Muller, the Genome Research Unit (Luxembourg Institute of Health), M. Zapatka, and Z. Huang, and the Core Facility Unit for high-throughput sequencing (DKFZ) for microarrays, small RNA sequencing, and bioinformatics analysis. The authors also thank Prof S. Niclou, A. Oudin, the Animal Facility, and N.H.C. Brons from the Flow Cytometry Facility (L.I.H.) for their help. The authors thank CLL patients and healthy donors who donated blood, Dr Schlesser, Dr François, and Prof Seil and his collaborators (Centre Hospitalier de Luxembourg) for clinical samples and Prof R. Bjerkvig (L.I.H.) for helpful discussion and Alexandra Casel (L.I.H.) for technical help.

This work was supported by Télévie (7.4504.11F), Fonds National de la Recherche-Luxembourg (C12/BM/3962058), and the German José Carreras Leukemia Foundation (DJCLS R 12/27). The Eric Solary team is supported by the Ligue Nationale Contre le Cancer and by grants from Institut National du Cancer and Agence Nationale de la Recherche (France).

Authorship

J.P. and E.M. designed the study, performed research, analyzed data, prepared figures, and wrote the paper; F.H., M.S., and P.L. performed next-generation sequencing analysis and analyzed data; U.D. and Y.J.K. performed mass spectrometry and analyzed data; W.A. performed exosome flow cytometry; J.A. performed immunohistochemistry staining; B.J., E.S., F.H., and M.S. wrote the paper; E.S. and G.B. supervised the study; and G.B. recruited patients.

Conflict-of-interest disclosure: The authors declare no competing financial interests.

The current affiliation for U.D. is Institute of Immunology, University Medical Center of the Johannes Gutenberg University of Mainz, Mainz, Germany.

Correspondence: Etienne Moussay and Jerome Paggetti, Laboratory of Experimental Hemato-Oncology, Luxembourg Institute of Health, 84 Val Fleuri, L-1526, Luxembourg, Luxembourg; e-mail: etienne.moussay@lih.lu and jerome.paggetti@lih.lu.

References

1. Damle RN, Calissano C, Chiorazzi N. Chronic lymphocytic leukaemia: a disease of activated monoclonal B cells. *Best Pract Res Clin Haematol.* 2010;23(1):33-45.
2. Martín-Subero JI, López-Otín C, Campo E. Genetic and epigenetic basis of chronic lymphocytic leukemia. *Curr Opin Hematol.* 2013; 20(4):362-368.
3. Damm F, Mylonas E, Cosson A, et al. Acquired initiating mutations in early hematopoietic cells of CLL patients. *Cancer Discov.* 2014;4(9): 1088-1101.
4. Kikushige Y, Ishikawa F, Miyamoto T, et al. Self-renewing hematopoietic stem cell is the primary target in pathogenesis of human chronic lymphocytic leukemia. *Cancer Cell.* 2011;20(2): 246-259.
5. Binsky I, Lantner F, Grabovsky V, et al. TAp63 regulates VLA-4 expression and chronic lymphocytic leukemia cell migration to the bone marrow in a CD74-dependent manner. *J Immunol.* 2010;184(9):4761-4769.
6. Scielzo C, Bertilaccio MT, Simonetti G, et al. HS1 has a central role in the trafficking and homing of leukemic B cells. *Blood.* 2010;116(18):3537-3546.
7. Tripodo C, Sangaletti S, Piccaluga PP, et al. The bone marrow stroma in hematological neoplasms–a guilty bystander. *Nat Rev Clin Oncol.* 2011;8(8):456-466.
8. Baginska J, Viry E, Paggetti J, et al. The critical role of the tumor microenvironment in shaping natural killer cell-mediated anti-tumor immunity. *Front Immunol.* 2013;4:490.
9. Théry C, Ostrowski M, Segura E. Membrane vesicles as conveyors of immune responses. *Nat Rev Immunol.* 2009;9(8):581-593.
10. Kulshreshtha A, Ahmad T, Agrawal A, Ghosh B. Proinflammatory role of epithelial cell-derived exosomes in allergic airway inflammation. *J Allergy Clin Immunol.* 2013;131(4):1194-1203.
11. Taylor DD, Gercel-Taylor C. MicroRNA signatures of tumor-derived exosomes as diagnostic biomarkers of ovarian cancer. *Gynecol Oncol.* 2008;110(1):13-21.
12. Valadi H, Ekström K, Bossios A, Sjöstrand M, Lee JJ, Lötvall JO. Exosome-mediated transfer of mRNAs and microRNAs is a novel mechanism of genetic exchange between cells. *Nat Cell Biol.* 2007;9(6):654-659.
13. Villarroya-Beltri C, Gutiérrez-Vázquez C, Sánchez-Cabo F, et al. Sumoylated hnRNPA2B1 controls the sorting of miRNAs into exosomes through binding to specific motifs. *Nat Commun.* 2013;4:2980.
14. Koppers-Lalic D, Hackenberg M, Bijnsdorp IV, et al. Nontemplated nucleotide additions distinguish the small RNA composition in cells from exosomes. *Cell Reports.* 2014;8(6): 1649-1658.
15. Zhang Y, Liu D, Chen X, et al. Secreted monocytic miR-150 enhances targeted endothelial cell migration. *Mol Cell.* 2010;39(1):133-144.
16. Umezu T, Ohyashiki K, Kuroda M, Ohyashiki JH. Leukemia cell to endothelial cell communication via exosomal miRNAs. *Oncogene.* 2013;32(22): 2747-2755.
17. Huan J, Hornick NI, Shurtleff MJ, et al. RNA trafficking by acute myelogenous leukemia exosomes. *Cancer Res.* 2013;73(2):918-929.
18. Umezu T, Tadokoro H, Azuma K, Yoshizawa S, Ohyashiki K, Ohyashiki JH. Exosomal miR-135b shed from hypoxic multiple myeloma cells enhances angiogenesis by targeting factor-inhibiting HIF-1. *Blood.* 2014;124(25):3748-3757.
19. Peinado H, Alečković M, Lavotshkin S, et al. Melanoma exosomes educate bone marrow progenitor cells toward a pro-metastatic phenotype through MET. *Nat Med.* 2012;18(6): 883-891.
20. Zhou W, Fong MY, Min Y, et al. Cancer-secreted miR-105 destroys vascular endothelial barriers to promote metastasis. *Cancer Cell.* 2014;25(4): 501-515.
21. Cols M, Barra CM, He B, et al. Stromal endothelial cells establish a bidirectional crosstalk with chronic lymphocytic leukemia cells through the TNF-related factors BAFF, APRIL, and CD40L. *J Immunol.* 2012;188(12):6071-6083.
22. Lutzny G, Kocher T, Schmidt-Supprian M, et al. Protein kinase c-β-dependent activation of NF-κB in stromal cells is indispensable for the survival of chronic lymphocytic leukemia B cells in vivo. *Cancer Cell.* 2013;23(1):77-92.
23. Öhlund D, Elyada E, Tuveson D. Fibroblast heterogeneity in the cancer wound. *J Exp Med.* 2014;211(8):1503-1523.
24. Madar S, Goldstein I, Rotter V. 'Cancer associated fibroblasts'–more than meets the eye. *Trends Mol Med.* 2013;19(8):447-453.
25. Moussay E, Palissot V, Vallar L, et al. Determination of genes and microRNAs involved in the resistance to fludarabine in vivo in chronic lymphocytic leukemia. *Mol Cancer.* 2010;9:115.
26. Moussay E, Wang K, Cho JH, et al. MicroRNA as biomarkers and regulators in B-cell chronic lymphocytic leukemia. *Proc Natl Acad Sci USA.* 2011;108(16):6573-6578.
27. Paggetti J, Berchem G, Moussay E. Stromal cell-induced miRNA alteration in chronic lymphocytic leukemia: how a minute and unavoidable cell contamination impairs miRNA profiling. *Leukemia.* 2013;27(8):1773-1776.
28. Moussay E, Kaoma T, Baginska J, et al. The acquisition of resistance to TNFα in breast cancer cells is associated with constitutive activation of autophagy as revealed by a transcriptome analysis using a custom microarray. *Autophagy.* 2011;7(7):760-770.
29. van der Vlist EJ, Nolte-'t Hoen EN, Stoorvogel W, Arkesteijn GJ, Wauben MH. Fluorescent labeling of nano-sized vesicles released by cells and subsequent quantitative and qualitative analysis by high-resolution flow cytometry. *Nat Protoc.* 2012;7(7):1311-1326.
30. Bertilaccio MT, Scielzo C, Simonetti G, et al. A novel Rag2-/-gammac-/–xenograft model of human CLL. *Blood.* 2010;115(8):1605-1609.

31. Hong CS, Muller L, Whiteside TL, Boyiadzis M. Plasma exosomes as markers of therapeutic response in patients with acute myeloid leukemia. *Front Immunol.* 2014;5:160.

32. Szajnik M, Derbis M, Lach M, et al. Exosomes in plasma of patients with ovarian carcinoma: potential biomarkers of tumor progression and response to therapy. *Gynecol Obstet (Sunnyvale).* 2013;(Suppl 4):3.

33. Christov CP, Gardiner TJ, Szüts D, Krude T. Functional requirement of noncoding Y RNAs for human chromosomal DNA replication. *Mol Cell Biol.* 2006;26(18):6993-7004.

34. Nolte-'t Hoen EN, van der Vlist EJ, Aalberts M, et al. Quantitative and qualitative flow cytometric analysis of nanosized cell-derived membrane vesicles. *Nanomedicine (Lond).* 2012;8(5): 712-720.

35. Navab R, Strumpf D, Bandarchi B, et al. Prognostic gene-expression signature of carcinoma-associated fibroblasts in non-small cell lung cancer. *Proc Natl Acad Sci USA.* 2011; 108(17):7160-7165.

36. Kalluri R, Zeisberg M. Fibroblasts in cancer. *Nat Rev Cancer.* 2006;6(5):392-401.

37. Kini AR, Kay NE, Peterson LC. Increased bone marrow angiogenesis in B cell chronic lymphocytic leukemia. *Leukemia.* 2000;14(8): 1414-1418.

38. Erez N, Truitt M, Olson P, Arron ST, Hanahan D. Cancer-Associated Fibroblasts Are Activated in Incipient Neoplasia to Orchestrate Tumor-Promoting Inflammation in an NF-kappaB-Dependent Manner. *Cancer Cell.* 2010;17(2): 135-147.

39. De Veirman K, Rao L, De Bruyne E, et al. Cancer associated fibroblasts and tumor growth: focus on multiple myeloma. *Cancers (Basel).* 2014;6(3): 1363-1381.

40. Li SJ, Chen HP, Chen YH, Zhang LH, Tu YM, Liu ZH. Renal involvement in non-Hodgkin lymphoma: proven by renal biopsy. *PLoS One.* 2014;9(4):e95190.

41. Uprety D, Peterson A, Shah BK. Renal failure secondary to leukemic infiltration of kidneys in CLL–a case report and review of literature. *Ann Hematol.* 2013;92(2):271-273.

42. Kucharzewska P, Christianson HC, Welch JE, et al. Exosomes reflect the hypoxic status of glioma cells and mediate hypoxia-dependent activation of vascular cells during tumor development. *Proc Natl Acad Sci USA.* 2013; 110(18):7312-7317.

43. Melo SA, Sugimoto H, O'Connell JT, et al. Cancer exosomes perform cell-independent microRNA biogenesis and promote tumorigenesis. *Cancer Cell.* 2014;26(5):707-721.

44. Hanahan D, Coussens LM. Accessories to the crime: functions of cells recruited to the tumor microenvironment. *Cancer Cell.* 2012;21(3): 309-322.

45. Pardoll DM. The blockade of immune checkpoints in cancer immunotherapy. *Nat Rev Cancer.* 2012; 12(4):252-264.

46. Kater AP, Tonino SH, Egle A, Ramsay AG. How does lenalidomide target the chronic lymphocytic leukemia microenvironment? *Blood.* 2014; 124(14):2184-2189.

47. Clayton A, Turkes A, Dewitt S, Steadman R, Mason MD, Hallett MB. Adhesion and signaling by B cell-derived exosomes: the role of integrins. *FASEB J.* 2004;18(9):977-979.

48. Christianson HC, Svensson KJ, van Kuppevelt TH, Li JP, Belting M. Cancer cell exosomes depend on cell-surface heparan sulfate proteoglycans for their internalization and functional activity. *Proc Natl Acad Sci USA.* 2013;110(43):17380-17385.

49. Alduaij W, Illidge TM. The future of anti-CD20 monoclonal antibodies: are we making progress? *Blood.* 2011;117(11):2993-3001.

50. Barrena S, Almeida J, Yunta M, et al. Aberrant expression of tetraspanin molecules in B-cell chronic lymphoproliferative disorders and its correlation with normal B-cell maturation. *Leukemia.* 2005;19(8):1376-1383.

51. Kumarswamy R, Volkmann I, Jazbutyte V, Dangwal S, Park DH, Thum T. Transforming growth factor-β-induced endothelial-to-mesenchymal transition is partly mediated by microRNA-21. *Arterioscler Thromb Vasc Biol.* 2012;32(2):361-369.

52. Li Q, Zhang D, Wang Y, et al. MiR-21/Smad 7 signaling determines TGF-β1-induced CAF formation. *Sci Rep.* 2013;3:2038.

53. Hsieh JY, Huang TS, Cheng SM, et al. miR-146a-5p circuitry uncouples cell proliferation and migration, but not differentiation, in human mesenchymal stem cells. *Nucleic Acids Res.* 2013;41(21):9753-9763.

54. Zhu K, Pan Q, Zhang X, et al. MiR-146a enhances angiogenic activity of endothelial cells in hepatocellular carcinoma by promoting PDGFRA expression. *Carcinogenesis.* 2013;34(9): 2071-2079.

55. Clayton A, Evans RA, Pettit E, Hallett M, Williams JD, Steadman R. Cellular activation through the ligation of intercellular adhesion molecule-1. *J Cell Sci.* 1998;111(Pt 4):443-453.

56. Schiappacassi M, Lovisa S, Lovat F, et al. Role of T198 modification in the regulation of p27(Kip1) protein stability and function. *PLoS One.* 2011; 6(3):e17673.

57. Binsky I, Haran M, Starlets D, et al. IL-8 secreted in a macrophage migration-inhibitory factor- and CD74-dependent manner regulates B cell chronic lymphocytic leukemia survival. *Proc Natl Acad Sci USA.* 2007;104(33):13408-13413.

58. Eksioglu-Demiralp E, Akdeniz T, Bayik M. Aberrant expression of c-met and HGF/c-met pathway provides survival advantage in B-chronic lymphocytic leukemia. *Cytometry B Clin Cytom.* 2011;80(1):1-7.

59. Kern C, Cornuel JF, Billard C, et al. Involvement of BAFF and APRIL in the resistance to apoptosis of B-CLL through an autocrine pathway. *Blood.* 2004;103(2):679-688.

60. Lafarge ST, Johnston JB, Gibson SB, Marshall AJ. Adhesion of ZAP-70+ chronic lymphocytic leukemia cells to stromal cells is enhanced by cytokines and blocked by inhibitors of the PI3-kinase pathway. *Leuk Res.* 2014;38(1):109-115.

61. Schulz A, Toedt G, Zenz T, Stilgenbauer S, Lichter P, Seiffert M. Inflammatory cytokines and signaling pathways are associated with survival of primary chronic lymphocytic leukemia cells in vitro: a dominant role of CCL2. *Haematologica.* 2011;96(3):408-416.

62. Simonetti G, Bertilaccio MT, Ghia P, Klein U. Mouse models in the study of chronic lymphocytic leukemia pathogenesis and therapy. *Blood.* 2014; 124(7):1010-1019.

63. Graves DT, Valente AJ. Monocyte chemotactic proteins from human tumor cells. *Biochem Pharmacol.* 1991;41(3):333-337.

64. Matsumura S, Wang B, Kawashima N, et al. Radiation-induced CXCL16 release by breast cancer cells attracts effector T cells. *J Immunol.* 2008;181(5):3099-3107.

65. Smith JB, Knowlton RP, Koons LS. Immunologic studies in chronic lymphocytic leukemia: defective stimulation of T-cell proliferation in autologous mixed lymphocyte culture. *J Natl Cancer Inst.* 1977;58(3):579-585.

66. Herishanu Y, Pérez-Galán P, Liu D, et al. The lymph node microenvironment promotes B-cell receptor signaling, NF-kappaB activation, and tumor proliferation in chronic lymphocytic leukemia. *Blood.* 2011;117(2):563-574.